Photosensitized Degradation of Dyes in Polyoxometalate Solutions Versus TiO_2 Dispersions under Visible-Light Irradiation: Mechanistic Implications

Chuncheng Chen,[a] Wei Zhao,[a] Pengxiang Lei,[a] Jincai Zhao,*[a] and Nick Serpone[b]

Abstract: This article examines the photoxidation of a dye (rhodamine-B, RhB) by visible-light irradiation in the presence of a polyoxometalate (12-tungstosilicic acid, $H_4SiW_{12}O_{40}$), and compares it with the analogous process in the presence of TiO_2. The photoreaction processes were examined by UV-visible spectroscopy, fluorescence spectroscopy, high-performance liquid chromatography (HPLC), liquid chromatography/mass spectral techniques (LC-MS), and total organic carbon (TOC) assays in order to identify the intermediates produced. Formation of oxygen species, such as H_2O_2 and $O_2^{\bullet-}$, was also investigated to clarify the details of the reaction pathway. With the use of $SiW_{12}O_{40}^{4-}$ ions as the photocatalyst, the photoreaction leads mainly to N-dealkylation of the chromophore skeleton. In contrast, cleavage of the whole conjugated chromophore structure predominates in the presence of TiO_2. Strong $O_2^{\bullet-}/HO_2^{\bullet-}$ ESR signals were detected in the TiO_2 dispersions, whereas only weak ESR signals for the $O_2^{\bullet-}$ radical ion were seen in the $SiW_{12}O_{40}^{4-}$ solutions during the irradiation period. Experimental results imply that reduction of O_2 occurs by different pathways in the two photocatalytic systems.

Keywords: photodegradation · polyoxometalates · reaction mechanisms · titanium oxide · visible-light irradiation

Introduction

Semiconductor photocatalysts, such as TiO_2, have gained much attention because they can potentially utilize inexpensive and inexhaustible solar radiation for environmental remediation. Moreover, they are useful in other diverse areas such as photo–electrochemical conversion to give energy, the photodissociation of water into H_2 and O_2,[1] the fixation of CO_2 and N_2,[2,3] and the photosynthesis of organic compounds.[4] Another class of photocatalytically active materials that have received somewhat less attention are the polyoxometalates (POMs).[5] Their unique combination of physical and chemical properties, in terms of molecular and electronic versatility, reactivity, and stability, make them a promising class of photocatalysts. Many POM systems share the same general photochemical characteristics as the semiconductor photocatalysts. For example, a variety of organic substrates can be oxidized photocatalytically, even mineralized, by POMs under UV irradiation (ca. $\lambda < 400$ nm).[6–13] A comparison of the photoxidation of organics by UV-illuminated POMs and semiconductors has also been reported.[7,14–16]

We set out to expand the useful response of semiconductor photocatalysts to visible light, and to investigate their potential application in the photodegradation of dye pollutants under visible irradiation. Towards this end, in recent years, we and others[17–21] have reported that various types of dyes can be photodegraded effectively in TiO_2 dispersions subjected to visible radiation. These systems were initiated by electron injection of the dyes in their excited state onto the conduction band of TiO_2. Certain polyoxometalates can also act as electron relays in a manner analogous to semiconductors such as TiO_2. In particular, they can undergo stepwise multi-electron redox reactions, while their structure remains intact. Substrates in highly reactive excited states should also transfer electrons to POMs in the ground state, and as a consequence become oxidized, while the POMs are reduced. Since POMs are important models in the elucidation of the photocatalytic action of metal–oxide semiconductors, investigations on the POM-assisted photodegradation of dyes by visible-light irradiation is expected to provide useful information for a greater understanding of both the photocatalysis reaction mechanism, and, more importantly, on the secondary events following the electron-transfer process. Moreover, to the extent that the photodegradation of dyes under visible-light irradiation in both TiO_2 and

[a] Dr. C. Chen, Dr. W. Zhao, Dr. P. Lei, Prof. J. Zhao
Laboratory of Photochemistry
Center for Molecular Science
Institute of Chemistry, Chinese Academy of Sciences
Beijing 100080 (China)
Fax: (+86) 10-8261-6495
E-mail: jczhao@iccas.ac.cn

[b] Prof. N. Serpone
Department of Chemistry and Biochemistry
Concordia University, 1455 de Maisonneuve Blvd West
Montreal, Quebec, H3G 1M8 (Canada)

DOI: 10.1002/chem.200305453

POM systems does not involve valence-band (VB) holes, it is an excellent probe by which to investigate the role of the reduced catalysts and dioxygen in the photocatalytic degradation of organic pollutants in both photocatalytic systems.

In this study, photodegradation of the rhodamine-B (RhB) dye mediated by visible-light irradiation of a POM

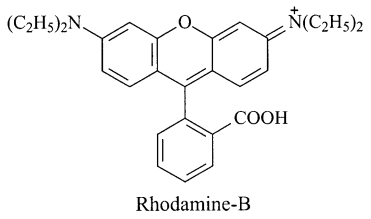

Rhodamine-B

($SiW_{12}O_{40}^{4-}$ ions) was examined for the first time. Differences in the photodegradative features of the $SiW_{12}O_{40}^{4-}$ and TiO_2 systems were also investigated in some detail. The aim of our present investigation was: 1) to uncover and assess the similarities and differences between the metal oxide semiconductor and the POM photocatalysts, 2) to provide a greater understanding of the reaction mechanism for the visible light induced degradation of dyes mediated by TiO_2, 3) to estimate the relative importance of O_2 in the photodegradation of organic compounds in both POM and TiO_2 systems, and 4) to explore the potential application of the selective oxidation and photosynthesis of POM-based photocatalytic processes when the POM is photosensitized by visible-light-irradiated dyes.

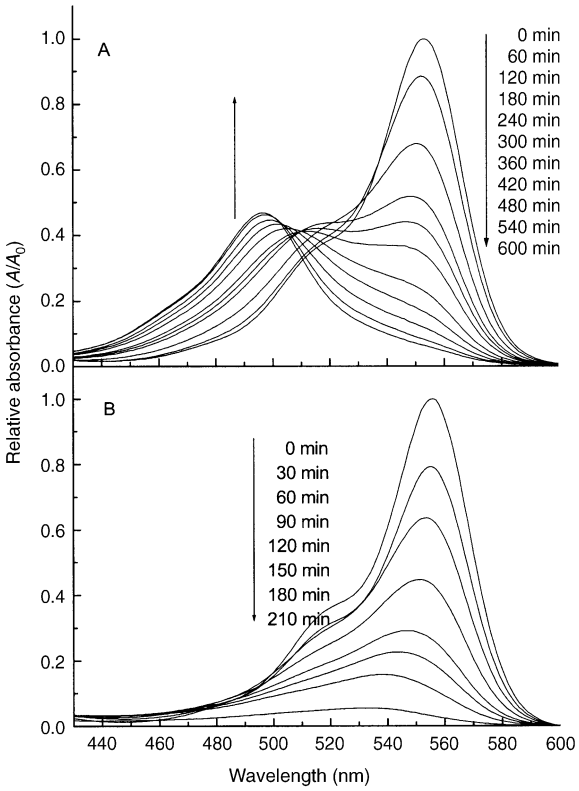

Figure 1. Temporal UV-visible absorption spectral changes observed for the RhB solutions as a function of irradiation time: A) in $SiW_{12}O_{40}^{4-}$ solutions (2×10^{-5} M); and B) in aqueous TiO_2 dispersions (TiO_2 loading of 1 g L^{-1}). Initial RhB concentration was 2×10^{-5} M at a pH of 2.5.

Results and Discussion

Separation and identification of the N-de-ethylated intermediate products of RhB: The target substrate RhB, which contains four *N*-ethyl groups at either side of the xanthene ring, is relatively stable in aqueous solutions upon visible-light irradiation. Furthermore, a reaction was not observed in the presence of either $SiW_{12}O_{40}^{4-}$ ions or TiO_2 when the reaction mixture was maintained in darkness. However, RhB underwent pronounced photodegradation in the presence of either of the two catalysts upon visible-light irradiation. The UV-visible spectral changes during the photodegradation of RhB in the presence of $SiW_{12}O_{40}^{4-}$ ions or TiO_2 are illustrated in Figures 1 A and B, respectively. The absorption maximum of the degraded solution at various times exhibited hypsochromic shifts to a certain extent; these resulted from the stepwise formation of a series of N-de-ethylated intermediates (see Figure 2 D below).

Direct evidence for the stepwise N-de-ethylation of RhB was demonstrated by LC-MS techniques. The typical HPLC chromatogram after visible-light irradiation in the presence of $SiW_{12}O_{40}^{4-}$ ions was recorded by both a UV-visible diode array detector (Figure 2 A, at 505 nm) and by a mass-spectral detector (Figure 2 B). The solution consisted of six HPLC components with retention times of less than 15 min. One of the peaks was the initial RhB dye (peak a). The other five peaks (b–f) were ascribed to intermediates. The relevant mass spectra, in which the molecular-ion peak of each intermediate is displayed, are illustrated in Figure 2 C. The molecular-ion peaks of the products differed exactly by 28 mass units in sequence; this is consistent with the sequential removal of the *N*-ethyl groups from the parent RhB molecule. The five different intermediates identified during the photoreaction were *N*,*N*-diethyl-*N*′-ethylrhodamine (DER), *N*-ethyl-*N*′-ethylrhodamine (EER), *N*,*N*-diethylrhodamine (DR), *N*-ethylrhodamine (ER), and rhodamine (R).

The absorption spectra of each intermediate in the visible spectral region are depicted in Figure 2 D. The spectra a (absorption maximum 550 nm), b (537 nm), c (522 nm), d (527 nm), e (512 nm), and f (500 nm) correspond to peaks a, b, c, d, e, and f in Figure 2 A and 2 B, respectively. The change in absorption maximum of the spectral bands (from 550 nm to 500 nm) corresponds to the hypsochromic shifts in Figure 1. The slight deviation in the absorption maxima between the spectra in Figure 1 (in aqueous media) and Figure 2 D (mixed aqueous methanolic media) is probably due to the nature of the solvent.

It is relevant to note that peaks c and d in Figure 2 display identical mass characteristics; this indicates that the intermediates contain two ethyl groups less than the RhB dye, and are isomeric. One of these isomers (EER) is formed by removal of an ethyl group from each side of the RhB molecule, whereas the other isomer (DR) is produced by removal

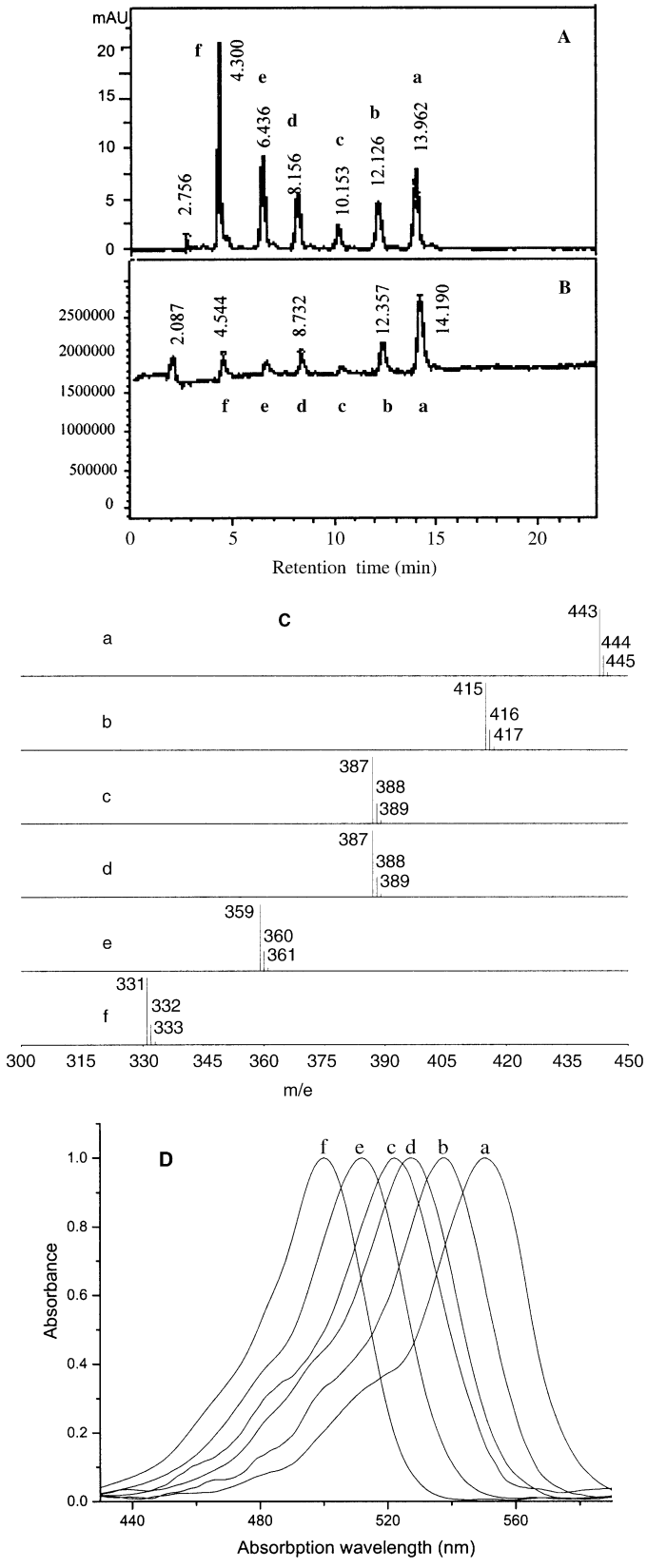

Figure 2. Typical HPLC chromatogram of the reaction solutions (A and B), the relevant mass spectra of the N-de-ethylated intermediates in which the molecular-ion peak of each intermediate formed is displayed (C), and UV-visible absorption spectra for each peak (D). The chromatograms were recorded by employing: A) a UV-visible diode array detector at 505 nm; and B) a mass-spectral detector.

of two ethyl groups from the same side of the RhB structure. If one considers that the polarity of the DR species is greater than that of the EER intermediate, the latter is expected to elute off the column after the DR species. Moreover, to the extent that two *N*-ethyl groups are stronger auxochromic moieties than an *N*,*N*-diethyl and an amido group, the maximum absorption for the DR (523 nm) intermediate is anticipated to occur at shorter wavelengths than the band position of the EER species (527 nm). Hence, peak d was assigned to DR, and peak c was attributed to EER. Most of the reports on oxidative N-de-ethylation of alkylamine showed that the alkyl group is transformed into an aldehyde. In our experiments, the fate of the ethyl groups in RhB were analyzed by mass-spectral techniques, and indicated that these groups were oxidized to acetaldehydes.

To confirm the structure of the intermediates, a typical intermediate (fully N-de-ethylated product R) was separated by repeated collection of the corresponding HPLC peak. The collected sample was further identified by high-resolution mass spectroscopy. The molecular mass was determined to be 331.1076480 with an error of only 1.846×10^{-7}; this is consistent with a fully N-de-ethylated RhB product (expected mass: 331.1077091).

After the initial amount of RhB (20 μM) had degraded in the presence of the $SiW_{12}O_{40}^{4-}$ ions (10 μM), the same amount of RhB was added again into the system. RhB decomposition in the second cycle was nearly as fast as in the first. Indeed, the POM did not display any significant loss of photoactivity in the four runs in which RhB was re-added. This indicates that the POM is fairly stable under the conditions used. In addition, the cycling experiment also implies that the photoreaction is a catalytic process rather than a stoichiometric one.

Comparison of the N-de-ethylated intermediates from RhB degradation mediated by $SiW_{12}O_{40}^{4-}$ ions and TiO_2: In the $SiW_{12}O_{40}^{4-}$ case, the hypsochromic shifts of the absorption maximum were rather significant. After irradiation for 600 min, the absorption band shifted from 553 nm to 497 nm (Figure 1 A). This evidence clearly indicates that N-de-ethylation predominates over the cleavage of the aromatic ring in the RhB dye. On the other hand, in the case of TiO_2 catalysis (Figure 1 B), the characteristic absorption band of the dye (around 553 nm) decreased rather rapidly (210 min), and new spectral features did not emerge even in the UV range ($\lambda > 200$ nm). These observations indicate that the whole conjugated chromophore structure of RhB undergoes facile cleavage in TiO_2 dispersions under visible irradiation. When the amount of TiO_2 was reduced to 0.1 gL^{-1}, degradation of the dye was considerably slower. However, significant hypsochromic shifts were not observed. Upon increasing the POM concentration to 400 μM, both the rate and extent of de-ethylation were nearly the same as in the 20 μM experiment. Clearly, this indicates that catalyst concentration cannot completely alter reaction pathways and intermediate distributions.

The distributions for all the N-de-ethylated intermediates in the presence of $SiW_{12}O_{40}^{4-}$ ions or TiO_2 at different irradiation times are illustrated in Figures 3 A and B, respective-

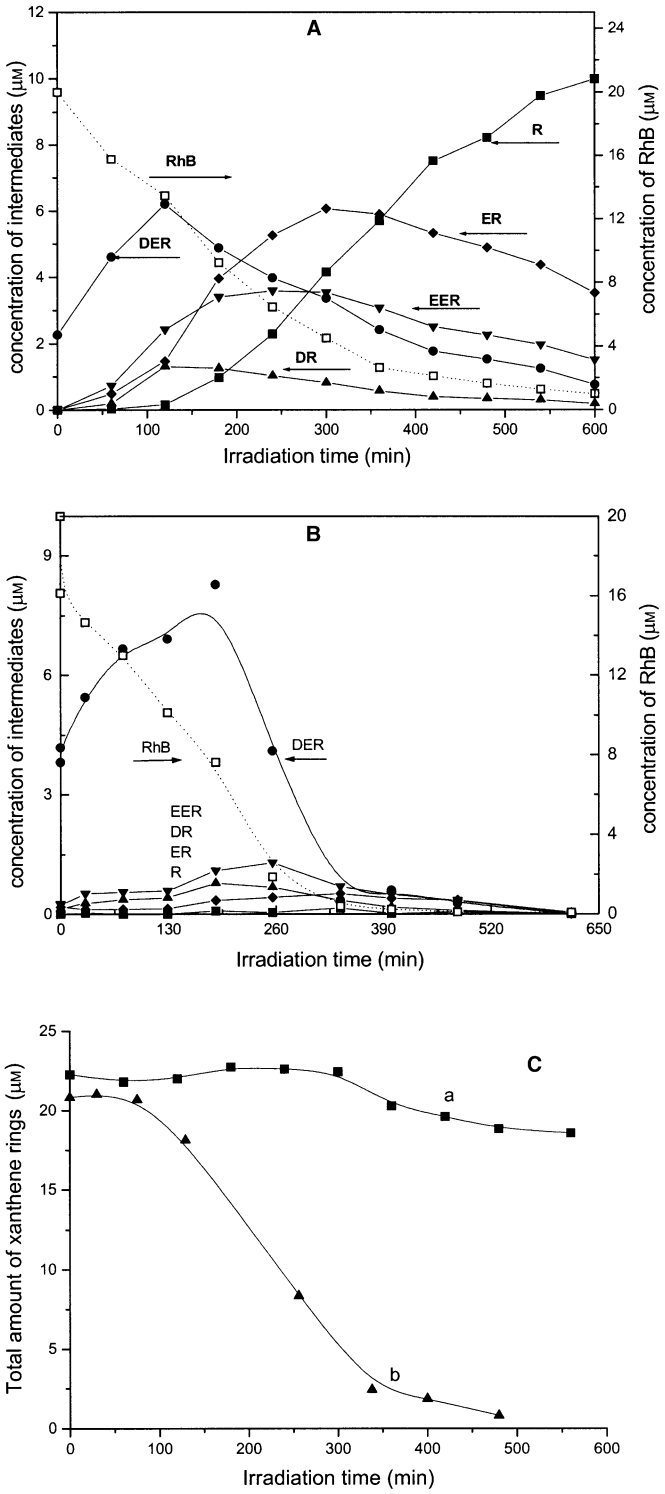

Figure 3. Variations in the distribution of the N-de-ethylated products from the photodegradation of RhB in the presence of $SiW_{12}O_{40}^{4-}$ (A) or TiO_2 (B), and the sum of the original RhB and its N-de-ethylated intermediates (total amount of xanthene rings) (C, curve a for $SiW_{12}O_{40}^{4-}$, and curve b for TiO_2) as a function of irradiation time.

ly. Except for the RhB dye and the fully de-ethylated product R, the other peaks increased and subsequently decreased; this indicates that the intermediates are transformed into other products after being formed.

The maximum yields of DER, EER, DR, and ER in the presence of $SiW_{12}O_{40}^{4-}$ ions, as estimated from individual molar-extinction coefficients, were 28%, 6%, 16%, and 32%, respectively. After ten hours of irradiation, the yield of the fully N-de-ethylated product R reached about 46%. However, unlike the other N-de-ethylated products, the amount of R did not decrease over the timescale of our experiments.

In the TiO_2 experiments, only the first mono-N-de-ethylated intermediate (DER) was clearly found in larger quantities (Figure 3B). However, unlike the $SiW_{12}O_{40}^{4-}$ system, other intermediates, not discussed as yet, were also detected, albeit to a much lesser extent. The sum of the original RhB and its N-de-ethylated intermediates (total amount of xanthene conjugated rings) in the two systems is depicted in Figure 3C, and indicates that the conjugated RhB structure is efficiently destroyed in TiO_2 dispersions (Figure 3C, curve b), while in $SiW_{12}O_{40}^{4-}$ solutions, cleavage of the conjugated structure occurs to a significantly lesser extent (Figure 3C, curve a). In accordance with these results, we deduced that de-ethylation of the RhB dye occurs to a rather small extent in the presence of TiO_2, and that the mineralization rate of RhB in TiO_2 dispersions is much greater than that observed in the presence of $SiW_{12}O_{40}^{4-}$ ions. This is also consistent with the results depicted in Figure 1 and 4.

Temporal TOC (total organic carbon) changes for RhB photodegradation in the two systems are depicted in Figure 4. In the $SiW_{12}O_{40}^{4-}$ system, the TOC values hardly

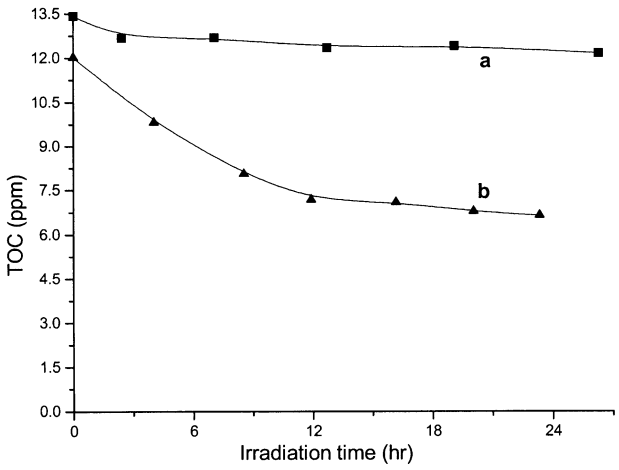

Figure 4. Temporal changes in total organic carbon (TOC) for the degraded bulk solution during RhB photodegradation (4×10^{-5} M; pH 2.5): a) $SiW_{12}O_{40}^{4-}$ (2×10^{-5} M); and b) TiO_2 (1 g L^{-1}).

changed after the photoreaction; this indicates that mineralization of the dye molecules occurs only to a negligible extent. However, in the TiO_2 dispersion, to the extent that dye molecules are adsorbed onto the TiO_2 surface, the TOC value of the bulk solutions at commencement was somewhat lower than that in the $SiW_{12}O_{40}^{4-}$ solutions. Under visible-light irradiation, TOC of the bulk solution for TiO_2 dispersions decreased gradually. After irradiation for 20 h, about 46% of TOC had been removed from the solution. The TOC remained unchanged after the dispersions were com-

pletely decolored; this indicates that the degraded fragments do not undergo any further decomposition upon further visible-light irradiation.

Formation of the reactive oxygen species: Reduced polyoxometalates are in many cases readily reoxidized, either by reaction with O_2 or H^+,[22] or with other oxidants such as metal ions[23] or halogenated alkanes.[24,25] Thus, the reduced POM is restored to its initial form, and the photocatalytic cycle is completed. Such a regeneration process (especially by O_2), which is regarded as a thermal dark reaction that occurs after the primary photochemical events, is key to the photomediated reactions of both systems.

The active oxygen species $O_2^{\bullet-}$/HOO$^\bullet$, H_2O_2, and $^\bullet$OH are those expected from reduction of O_2, and are accompanied by reoxidation of the photocatalysts. Formation of a superoxide radical anion was examined by electron-spin resonance (ESR)/DMPO (DMPO = 5,5-dimethyl-1-pyrroline-*N*-oxide) spin-trapping techniques in methanolic media, because the facile disproportionation of the superoxide species in water[26] precludes the slow reactions between $O_2^{\bullet-}$ or $^\bullet$OOH and DMPO ($k = 10$ and $6.6\times10^3\,\text{M}^{-1}\text{s}^{-1}$, respectively).[27] During laser irradiation at 532 nm, relatively strong signals for DMPO–$O_2^{\bullet-}$ adducts appeared in the TiO_2 dispersions (Figure 5B). In contrast, under otherwise identical conditions, a weak set of $O_2^{\bullet-}$ signals emerged for the $SiW_{12}O_{40}^{4-}$ solutions (Figure 5A).

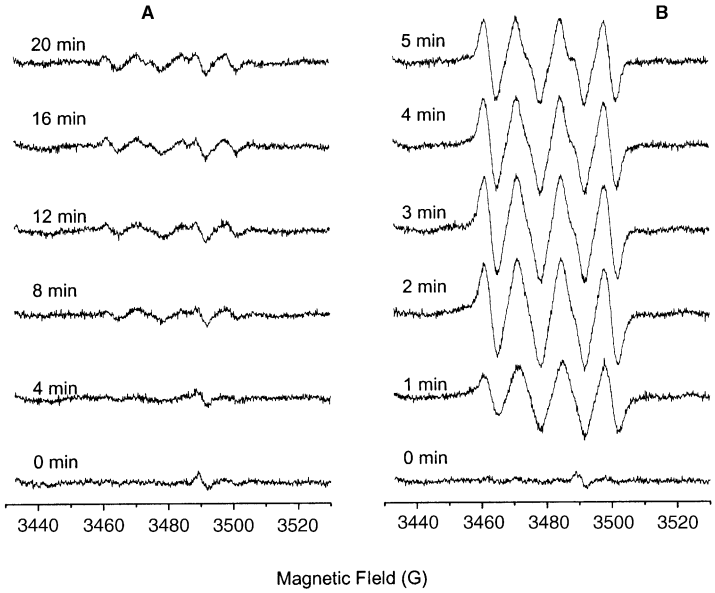

Figure 5. ESR spectra for the superoxide radical ($O_2^{\bullet-}$/$^\bullet$OOH) adducts with DMPO after different periods of irradiation with a pulsed laser (λ = 532 nm, 10 Hz): A) RhB (4×10^{-5} M)/$SiW_{12}O_4^{4-}$ solution (2×10^{-5} M); and B) RhB (4×10^{-5} M)/TiO_2 dispersion (2 g L^{-1}).

The amount of H_2O_2 detected during the irradiation period depends on both its rate of formation and its rate of decomposition. In TiO_2 dispersions, H_2O_2 can be produced from disproportionation of the superoxide radical [Eqs. (1) and (2)] or from the superoxide radical receiving another electron and two protons [Eq. (3)].[26,28–30] On the other hand, decomposition of H_2O_2 can occur by the addition of an electron from the reduced catalysts [Eq. (4)]. These reactions can be regarded as a quasi-serial type for which a maximum concentration is expected.

$$e^- + O_2 \rightarrow O_2^{\bullet-} \quad (1)$$

$$2\,O_2^{\bullet-} + 2\,H^+ \rightarrow H_2O_2 + O_2 \quad (2)$$

$$O_2^{\bullet-} + e^- + 2\,H^+ \rightarrow H_2O_2 \quad (3)$$

$$H_2O_2 + e^- \rightarrow OH^- + {}^\bullet OH \quad (4)$$

Formation of H_2O_2 during the photoreaction in $SiW_{12}O_{40}^{4-}$ solutions or TiO_2 dispersions was determined by *N*,*N*-dialkyl-*p*-phenylenediamine (DPD) spectrometric methods. The temporal profiles of H_2O_2 concentration against irradiation time are illustrated in Figure 6. In both $SiW_{12}O_{40}^{4-}$/RhB solutions and the TiO_2/RhB suspensions, the maximal amounts of H_2O_2 were 19 and 19.5 μM, respectively. We fitted kinetic curves that employ the consecutive reaction mode to estimate qualitatively the rates of their formation and degradation. Fitted apparent rate constants are $k_1 = 1.81\times10^{-3}\,\text{min}^{-1}$ and $k_2 = 1.61\times10^{-3}\,\text{min}^{-1}$ for the POM system, and $k_1 = 4.14\times10^{-3}\,\text{min}^{-1}$ and $k_2 = 3.38\times10^{-3}\,\text{min}^{-1}$ for the TiO_2 dispersion. This indicates that both the rates of formation and decomposition of H_2O_2 in the TiO_2 dispersion are greater than those in the POM system.

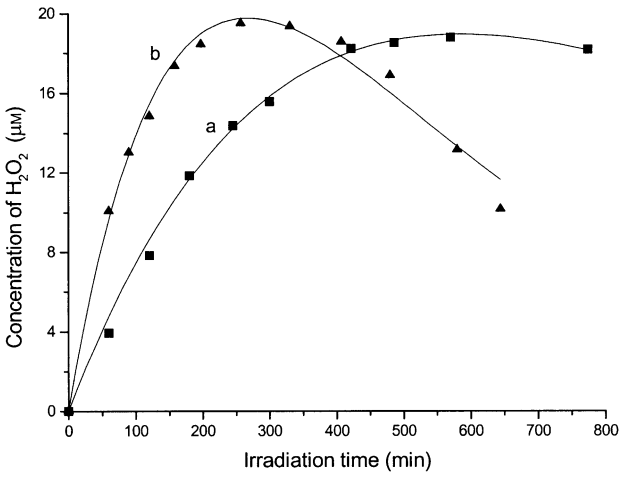

Figure 6. Concentration profiles for the formation of H_2O_2 during RhB (2×10^{-5} M) photodegradation under visible-light irradiation in the presence of: a) $SiW_{12}O_{40}^{4-}$ ions (2×10^{-5} M); and b) TiO_2 particles (1 g L^{-1}).

During TiO_2-assisted degradation of the dye under visible-light irradiation, the formed H_2O_2 is able to gain another conduction-band electron to produce a hydroxyl radical [Eq. (4)]. The $^\bullet$OH radical is a rather reactive species that degrades many classes of organic substrates. However, addition of a 0.2 mM solution of H_2O_2 to the TiO_2 dispersions had only a weak effect on the degradation of the dye, even though the added H_2O_2 was efficiently decomposed. The addition of a catalase (22 ppm) that catalyzes the dismutation

of H_2O_2 into H_2O and O_2 also influenced the degradation only to a small extent. This implies that H_2O_2 plays only a minor role in the degradation of RhB in TiO_2 dispersions.

In the $SiW_{12}O_{40}^{4-}$ system, the formation of a considerable amount of H_2O_2 during irradiation (Figure 6, curve a) seems somewhat strange, since only a small amount of $O_2^{\bullet-}$ was detected. In accord with our present results, Papaconstantinou and Hiskia[31] suggested that dioxygen acts as a two-electron-transfer oxidant and that H_2O_2 is in fact the resultant product. They further showed that reoxidation of POM by H_2O_2 is rather slow (about 24 times slower than by O_2). These observations imply that H_2O_2 is derived directly from the coordinated O_2 or coordinated $O_2^{\bullet-}$ ion by addition of an electron and subsequent facile dissociation from the polyoxometalate anion. Therefore, we added H_2O_2 (0.2 mM) and catalase (22 ppm) to two separate $SiW_{12}O_{40}^{4-}$ systems. Although the added H_2O_2 can be degraded under turnover conditions, it changed the reaction rates of RhB degradation only slightly. Moreover, addition of catalase also influenced the degradation only to a small extent. This indicates that the H_2O_2 formed during irradiation plays only a minor role in the N-de-ethylation of RhB in POM solutions.

The effect of superoxide dismutase (SOD) on the RhB degradation rates in both systems is illustrated in Figure 7.

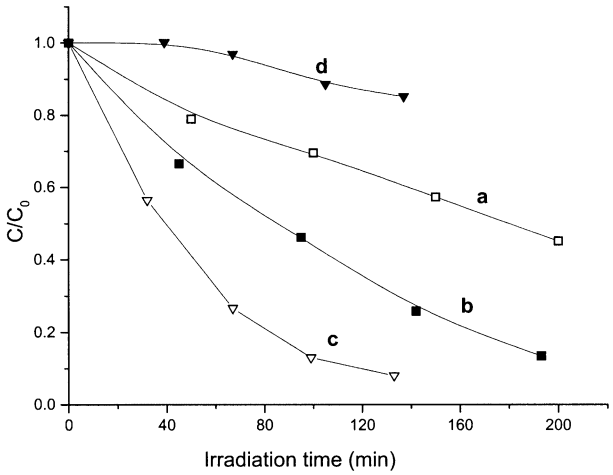

Figure 7. Normalized concentration profiles showing RhB degradation kinetics upon addition of SOD (10000 Units): a) $SiW_{12}O_{40}^{4-}$/RhB; b) $SiW_{12}O_{40}^{4-}$/RhB/SOD; c) TiO_2/RhB; and d) TiO_2/RhB/SOD.

The presence of SOD (ca. 10000 Units), which catalyzes the dismutation of $O_2^{\bullet-}$, can significantly accelerate removal of RhB (Figure 7, curve b), and greatly enhances the hypsochromic shifts displayed in the spectra of the $SiW_{12}O_{40}^{4-}$ solutions. In contrast, the presence of SOD in the TiO_2 dispersions led to a marked suppression of RhB photodegradation (Figure 7, curve d) in which the rate constant dropped markedly. It is unlikely that this suppression resulted from a decrease in the adsorption of RhB onto the surface of TiO_2 as addition of SOD did not cause any significant variation in RhB adsorption.

Interactions between the photocatalyst ($SiW_{12}O_{40}^{4-}$ ions or TiO_2) and the RhB dye: Polyoxometalates can interact with substituted amides[32] and aromatic amines[33] through the nitrogen atoms to produce novel hybrid materials. In many investigations that involved POMs, the alkylammonium cation was the counterion for the polyoxometalate salt. The RhB dye also contains two *N*,*N*-diethyl groups. Therefore, this dye should be able to interact with the negatively charged $SiW_{12}O_{40}^{4-}$ ions. Interactions between the POM and RhB were evidenced by a remarkable change in the absorption spectra (Figure 8A), and by the dramatic quenching of the

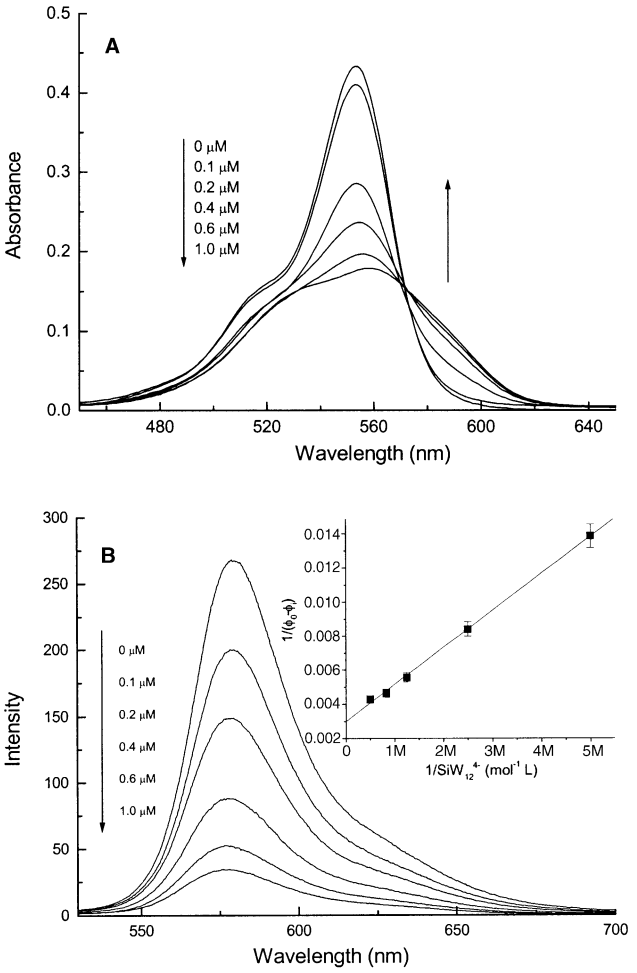

Figure 8. Changes in the absorption spectra (A) and fluorescence spectra excited at $\lambda_{ex}=500$ nm (B) of rhodamine B (RhB) solutions in the presence of different concentrations of $H_4SiW_{12}O_{40}$. The inset in B shows the dependence of $1/(\Phi_0-\Phi_i)$ on the reciprocal concentration of the $SiW_{12}O_{40}^{4-}$ ion. Φ_0 is the fluorescence quantum yield of RhB in the absence of catalyst, whereas Φ_i denotes the quantum yield in the presence of $SiW_{12}O_{40}^{4-}$ ions at various concentrations.

fluorescence of RhB upon addition of $SiW_{12}O_{40}^{4-}$ ions to the solution (Figure 8B). On the basis of dye-fluorescence intensity changes, the apparent association constant was estimated from a Benesi–Hildebrand-type plot (inset of Figure 8B)[34,35] to be $1.37\times10^6\,M^{-1}$.

Other cationic dyes, such as malachite green (MG), also undergo degradation by visible irradiation in the presence of $SiW_{12}O_{40}^{4-}$ ions. The anionic dye *N*,*N*,*N*′,*N*′-tetraethylsulforhodamine (SRB), which scarcely interacts with the $SiW_{12}O_{40}^{4-}$ ion, does not undergo substantial photoreaction

with SRB, even after ten hours of visible-light irradiation. From this, it can be concluded that a POM–RhB interaction is necessary for a photoreaction to take place.

A structural characteristic of the RhB dye is that it is dipolar. That is, it contains positively charged diethylamine groups and a negatively charged carboxylate group at different positions in the dye molecule. The carboxylate group can easily be adsorbed onto the surface of TiO_2, because the latter are positively charged in acidic media.[36] Although the sterically bulky xanthene ring (see RhB structure above) somewhat hampers the negatively charged group from reaching the TiO_2 surface particles, a slight red-shift (~1 nm in 2 g L^{-1} TiO_2) of the absorption maximum was observed upon addition of colloidal TiO_2. This indicates that the interaction between TiO_2 and the dye is relatively weak. Nonetheless, carboxylate groups can effectively adsorb onto a metal oxide surface, as evidenced in dye-sensitized solar cells (e.g., the Graztel cell), which act as a bridge for the electron-injection process.[37–39]

Proposed reaction pathways: For oxidative N-dealkylation of alkylamine in POM systems under UV irradiation ($\lambda <$ 400 nm), the proposed pathway involves H atom abstraction from the α-carbons followed by capture of the resultant radicals with O_2 and subsequent de-ethylation.[11,12,15] This pathway does not seem to apply for visible irradiation, as it is the dye rather than the POM that is excited. The "transient X" species, which is generated by excitation of the POM by UV irradiation, and which is regarded as the primary species for the H atom abstraction, is not formed under visible irradiation. Previous investigations in which electrochemical, enzymatic, and photochemical methods were used, tended to support a mechanism that involves electron transfer and deprotonation.[40,41] Hence, de-ethylation of RhB in the presence of $SiW_{12}O_{40}^{4-}$ ions is initiated by excitation of the dye, and is followed by electron transfer to the LUMOs of the $SiW_{12}O_{40}^{4-}$ ions. This theory is further supported by the following evidence obtained from our experiments: 1) the redox potential of the $SiW_{12}O_{40}^{4-}$ ion [+0.05 V versus normal hydrogen electrode (NHE)],[6,31] which is more positive than that of the excited state of the dye (RhB*, −1.4 V versus NHE), favors electron transfer from the excited dye to the LUMO of the $SiW_{12}O_{40}^{4-}$ anions; 2) $SiW_{12}O_{40}^{4-}$ ions can serve as multi-electron relays; 3) interactions between the photocatalyst and the dye make the electron-transfer event possible; and 4) the electron transfer between the dye and $SiW_{12}O_{40}^{4-}$ ions can be further confirmed by the fact that fluorescence is quenched (Figure 8B).

Since electron injection from the excited RhB dye to the respective ground states of the two photocatalysts is generally analogous, and catalyst concentration cannot change the whole reaction pathway, the differences in the intermediate yields and the mineralization rates observed between the $SiW_{12}O_{40}^{4-}$ ions and TiO_2 are likely to be caused by secondary chemical events that occur after visible-light-induced electron injection.

Both outer- and inner-sphere mechanisms have been proposed for the reoxidation of the reduced POMs by dioxygen. In the outer-sphere reduction of dioxygen, the reduced POM transfers an electron to O_2 to form the expected free $O_2^{\bullet-}$ radical ions. This mechanism is strongly supported by the elegant ^{17}O-labeling studies of Duncan and Hill in which O_2 incorporation into the POM anions was not observed.[42] However, the authors do acknowledge that, because the oxygen-exchange chemistry of hypothetical POM–O_2 adducts could not be appraised, such an absence did not entirely preclude an operational inner-sphere mechanism.

An inner-sphere electron transfer that involves covalently bonded M−O intermediates has been proposed by Hiskia et al.[31] and Neumann et al.[43] In this mechanism, the dioxygen either becomes associated to the tungsten atom to form a seven-coordinate metal center (Scheme 1, reaction 5,

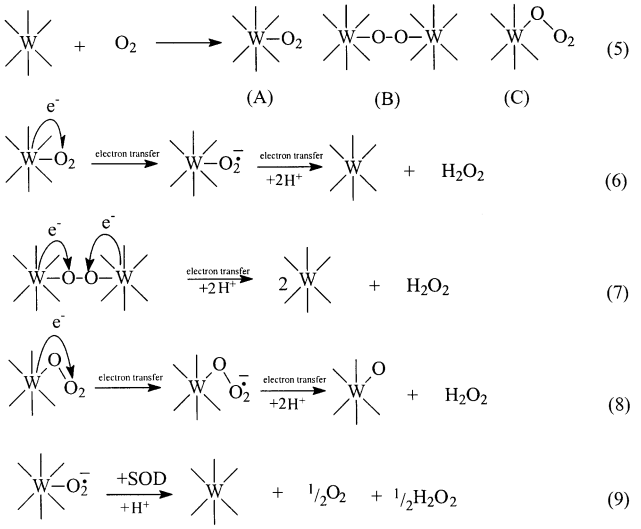

Scheme 1. Inner-sphere mechanism for reoxidation of the reduced polyoxotungstate by molecular oxygen.

structure A and B), or is added to the terminal oxygen atom to form an ozonide (Scheme 1, reaction 5, structure C). Heteropolyperoxotungstate salts that contain seven-coordinate W atoms linked to oxygen atoms have been synthesized,[44,45] and provide further evidence that inner-sphere coordination between the POM and O_2 is possible.

In keeping with an inner-sphere electron-transfer mechanism, under our experimental conditions, very small amounts of free $O_2^{\bullet-}$ were detected during visible irradiation of $SiW_{12}O_{40}^{4-}$/RhB solutions (Figure 5). Moreover, the redox potential of the $SiW_{12}O_{40}^{4-}$ ions (+0.05 V versus NHE[6,31]) is more positive than that of O_2 (−0.05 V versus NHE at 1 unit pressure of O_2 and at pH 0[26]). Therefore, from a thermodynamic point of view, electron transfer from the reduced $SiW_{12}O_{40}^{5-}$ system to O_2 is unlikely to occur. However, the redox potential of O_2/H_2O_2 (+0.72 V versus NHE at 1 atm of O_2 and at pH 7) is more positive than that of the POM, so it is possible that O_2 is reduced to H_2O_2 by the reduced POM through a two-electron-transfer process. Coordination between the POM (more probably the reduced POM) and O_2 could make an inner-sphere two-electron transfer likely. In this pathway, little if any free superoxide radical anions would be formed, but coordinated $O_2^{\bullet-}$ radical ions can be formed as a result of a one-electron

transfer from the POM to the O_2 moiety in the $SiW_{12}O_{40}^{4-}$–O_2 complexes (Scheme 1, reactions 6–8). Addition of SOD can also lead to the dismutation of a coordinated $O_2^{\bullet-}$ species to give H_2O_2 and O_2 (Scheme 1, reaction 9). As a result, SOD can enhance the charge separation and accelerate the rates of RhB N-de-ethylation (Figure 7, curve b).

Formation of $O_2^{\bullet-}$ radical ions in TiO_2 dispersions under both visible and UV-light irradiation is suggested from the degraded organic intermediates,[46,47] and detected by ESR spin-trapping or chemiluminescence methods.[48–51] In our experiments, strong $O_2^{\bullet-}$ signals were also observed in the TiO_2 dispersions during visible-light irradiation (Figure 5B); this indicates that the conduction-band electrons are trapped by dioxygen through an outer-sphere electron-transfer pathway; that is, mobile $O_2^{\bullet-}$ species are formed as a result of O_2 reduction.

Photoreaction was slower in de-aerated solutions, but was by no means eliminated completely in the POM system; this indicates that a redox reaction between the excited dye and the POM is able to occur. However, in the TiO_2 dispersions, a reaction was not observed in the absence of O_2; this is consistent with the earlier investigations carried out under UV irradiation,[14] and suggests that O_2 plays a very important role in the photoreactions of both systems. The role of O_2 in the photo-assisted degradations of organic compounds is twofold: 1) it suppresses charge recombination and regenerates the photocatalysts by acting as an electron acceptor and 2) it participates directly in the chemical oxidation of substrates through active oxygen species and/or ground state O_2. Most investigations into photocatalytic processes that involve both polyoxometalates and TiO_2 have indicated that O_2 primarily takes on the former function. Only recently, have studies reported the requisite conditions for O_2 to take on the latter role in TiO_2-assisted photodegradation of aromatic compounds under UV irradiation.[29,30,46] Under UV irradiation, excitation of TiO_2 leads to the formation of conduction-band electrons and valence-band holes. However, in the degradation of dyes under visible irradiation, injection of electrons from the dye into the catalyst also results in the formation of conduction-band electrons. Although the mechanistic details of the degradation of dyes under visible irradiation differ greatly from those in the photodegradation of organic compounds under UV irradiation, there should be very little, if any, difference in the manner by which photogenerated electrons are scavenged by O_2, or how $O_2^{\bullet-}$ radical ions are formed. Recently, we suggested that O_2 is essential for the photodegradation of dyes under visible-light irradiation, and in fact, cannot be substituted by other electron acceptors.[52] By considering the intrinsic and nonselective character of reactive oxygen radical species such as $O_2^{\bullet-}$, and the manner in which SOD suppresses RhB degradation in TiO_2 dispersions (Figure 7, curve d), we infer that $O_2^{\bullet-}$ plays an important role in the degradation of dyes in TiO_2 dispersions. In particular, cleavage of the RhB chromophore structure is attributed to attack of the dye (more possibly its radical cations) by $O_2^{\bullet-}$/$^{\bullet}OOH$ ions.[29,30,46,47] The differences in the photoreaction mechanism between the two systems are summarized in Scheme 2 (reactions 10–16).

$$RhB \longrightarrow RhB^* \quad (10)$$

In TiO_2 dispersions:

$$RhB^* + TiO_2 \longrightarrow TiO_2(e^-) + RhB^{+\bullet} \quad (11)$$

$$TiO_2(e^-) + O_2 \longrightarrow TiO_2 + O_2^{-\bullet} \quad (12)$$

$$RhB^{+\bullet}(RhB) + O_2^{-\bullet} \longrightarrow \text{structure cleavage} \quad (13)$$

In POM system:

$$RhB^* + POM \longrightarrow POM^- + RhB^{+\bullet} \quad (14)$$

$$POM^- + O_2 + H^+ \longrightarrow POM + H_2O_2 \quad (15)$$

$$RhB^{+\bullet} \longrightarrow N\text{-de-ethylated products} \quad (16)$$

Scheme 2. Proposed differences in the photocatalytic degradation pathways of RhB by TiO_2 and POM.

Conclusion

The RhB dye undergoes effective photoreaction under visible-light irradiation in the presence of both $SiW_{12}O_{40}^{4-}$ ions and TiO_2 as photocatalysts. With $SiW_{12}O_{40}^{4-}$ ions as the photocatalyst, the photoreaction leads mainly to N-dealkylation of the chromophore skeleton. In contrast, in the presence of TiO_2, cleavage of the whole conjugated chromophore structure predominates. The mobility of the $O_2^{\bullet-}$ species, which is formed by reoxidation of the reduced catalysts by molecular oxygen, accounts for the differences. In the POM system, according to the inner-sphere reoxidation mechanism, only a small quantity of free mobile $O_2^{\bullet-}$ is produced, while the majority of O_2 undergoes a two-electron-transfer reductive process to yield H_2O_2 directly. Moreover, the dye radical cations can lose one ethyl group upon hydrolysis. In contrast, in the TiO_2 system, formation of free $O_2^{\bullet-}$ radical ions leads to mineralization of the dye.

Experimental Section

Materials: The $H_4SiW_{12}O_{40}\cdot H_2O$ catalyst used in this study was prepared and purified according to literature procedure.[53] Titanium dioxide (TiO_2) (particles P25; ca. 80% anatase, 20% rutile; BET specific surface area, ca. 50 m^2g^{-1}) was kindly supplied by Degussa. Horseradish peroxidase (POD), which was used to assess the quantity of H_2O_2 produced, was obtained from the Huamei Biologic Engineering Co. (China), whereas DPD was obtained from Merck. The rhodamine-B dye (RhB) was of laser-grade quality. All other chemicals were of analytical reagent grade, and were used without further purification. De-ionized and doubly distilled water was used throughout this study. The pH of the solutions was adjusted with dilute aqueous solutions of either NaOH or $HClO_4$.

Photoreactor and light source: A 500 W halogen lamp (Institute of Electric Light Source, Beijing) was positioned inside a cylindrical Pyrex reactor, which was surrounded by a circulating water jacket (Pyrex) to cool the lamp and minimize infrared radiation. A cut-off filter was placed outside the Pyrex jacket to completely eliminate any radiation at wavelengths below 420 nm, and thereby, to ensure that illumination occurred only from visible light ($\lambda > 420$ nm).

Procedures and analyses: The aqueous RhB/TiO_2 dispersions were typically prepared by addition of TiO_2 (P25, 25 mg) to an aqueous solution (25 mL) of RhB dye (2×10^{-5} M). Prior to irradiation, the suspensions were magnetically stirred in the dark for about 30 min to ensure that a

suitable adsorption/desorption equilibrium of the dye on the surface of TiO_2 had been established. Unless noted otherwise, the dispersions were kept under constant air-equilibrated conditions before and during irradiation. At given time intervals, aliquots (3 mL) were sampled, centrifuged, and then filtered through a Millipore filter (pore size 0.22 μm) to remove the TiO_2 particles. The filtrates were analyzed by a Lambda Bio 20 spectrophotometer (Perkin–Elmer), which recorded the temporal UV-visible spectral variations of the dyes. In the $SiW_{12}O_{40}^{4-}$ systems, the solution (25 mL) of dye (2×10^{-5} M) and $SiW_{12}O_{40}^{4-}$ (2×10^{-5} M) at pH 2.5 was illuminated under aerated conditions. At given time intervals, aliquots (3 mL) were sampled, buffered to pH 9 by the addition of a Na_2CO_3/$NaHCO_3$ solution (1 mL), and subsequently analyzed by HPLC or UV-visible spectroscopy. The concentration of H_2O_2 formed during the irradiation was determined by the spectrophotometric DPD method[37] immediately after irradiation. The consecutive reaction mode [Eq. (17)] was employed to fit the kinetic curves and to estimate the apparent formation and decomposition rate constants of H_2O_2 in both systems.

$$[H_2O_2] = \frac{Ak_1}{k_2-k_1}(e^{k_1t}-e^{k_2t}) \quad (17)$$

Fluorescence spectra were recorded on an F-4500 spectrofluorimeter, whereas the diffuse-reflectance spectra were recorded on a Hitachi UV-3900 spectrophotometer equipped with an integrating sphere attachment. Barium sulfate was used as the reflectance standard.

The N-dealkylated intermediates and the original dye were identified by an Agilent 1100 LC-MSD Trap system (LC-MS). The solution gradient was regulated by water and methanol (from 60% to 90% methanol over 25 min). The intermediates were quantified by a Dionex HPLC system (Dionex P580 pump and a UVD 340S diode-array detector) using an ammonium phosphate buffer solution (0.1%, v/v) and methanol as the eluent (from 60% to 90% methanol over 15 min). In both cases, an Intersil ODS-3C-18 reverse-phase column was employed. A pure sample of each fully de-ethylated intermediate was isolated by repeated collection of the corresponding HPLC peak, and the structures were confirmed by high-resolution mass spectroscopy (APEX II, FT-ICRMS, Bruker Daltonics). Total organic carbon (TOC) assays were carried out on a Tekmar Dohrmann Apollo 9000 TOC analyzer.

Acknowledgements

Generous financial support from the Ministry of Science and Technology of China (No. 2003CB415006), the National Science Foundation of China, and the Chinese Academy of Sciences is gratefully acknowledged. The studies in Montreal were sponsored by the Natural Sciences and Engineering Research Council of Canada.

[1] K. Honda, A. Fujishima, *Nature* **1972**, *238*, 37–38.
[2] T. Inoue, A. Fujishima, S. Konishi, K. Honda, *Nature* **1979**, *277*, 637–638.
[3] a) G. N. Schrauzer, T. D. Guth, *J. Am. Chem. Soc.* **1977**, *99*, 7189–7193; b) O. Rusina, O. Linnik, A. Eremenko, H. Kisch, *Chem. Eur. J.* **2003**, *9*, 561–565; c) K. Hoshino, M. Inui, T. Kitamura, H. Kokado, *Angew. Chem.* **2000**, *112*, 2558–2561; *Angew. Chem. Int. Ed.* **2000**, *39*, 2509–2512.
[4] R. Künneth, C. Feldmer, H. Kisch, *Angew. Chem.* **1992**, *104*, 1102–1103; *Angew. Chem. Int. Ed. Engl.* **1992**, *31*, 1039–1040.
[5] R. R. Ozer, J. L. Ferry, *J. Phys. Chem. B* **2002**, *106*, 4336–4342.
[6] I. A. Weinstock, *Chem. Rev.* **1998**, *98*, 113–170.
[7] A. Hiskia, A. Mylonas, E. Papaconstantinou, *Chem. Soc. Rev.* **2001**, *30*, 62–69.
[8] R. R. Ozer. J. L. Ferry, *J. Phys. Chem. B* **2000**, *104*, 9444–9448.
[9] E. Androulaki, A. Hiskia, D. Dimotikali, C. Minero, P. Calza, E. Pelizzetti, E. Papaconstantinou, *Environ. Sci. Technol.* **2000**, *34*, 2024–2028.
[10] A. Maldotti, R. Amadelli, G. Varani, S. Tollari, F. Porta, *Inorg. Chem*, **1994**, *33*, 2968–2973.
[11] C. Tanielian, K. Duffy, A. Jones, *J. Phys. Chem. B* **1997**, *101*, 4276–4282.
[12] D. C. Duncan, M. A. Fox, *J. Phys. Chem. A* **1998**, *102*, 4559–4567.
[13] S.-F. Jen, A. B. Anderson, C. L. Hill, *J. Phys. Chem.* **1992**, *96*, 5658–5662.
[14] R. C. Chambers, C. L Hill, *Inorg. Chem.* **1991**, *30*, 2776–2781.
[15] I. Texier, J. Ouazzani, J. Delaire, C. Giannotti, *Tetrahedron* **1999**, *55*, 3401–3412.
[16] I. Texier, C. Giannotti, S. Malato, C. Richter, J. Delaire, *Catal. Today* **1999**, *54*, 297–307.
[17] F. Zhang, J. Zhao, H. Hidaka, E. Pelizzetti, N. Serpone, *Appl. Catal. B* **1998**, *15*, 147–156.
[18] T. Wu, G. Liu, J. Zhao, H. Hidaka, N. Serpone, *J. Phys. Chem. B* **1998**, *102*, 5845–2851
[19] G. Liu, X. Li, J. Zhao, H. Hidaka, N. Serpone, *Environ. Sci. Technol.* **1999**, *33*, 2081–2087
[20] G. Liu, X. Li, J. Zhao, H. Hidaka, N. Serpone, *Environ. Sci. Technol.* **2000**, *34*, 3982–3900.
[21] A. B. Prevot, C. Baiocchi, M. C. Brussino, E. Pramauro, P. Savarino, V. Augugliaro, G. Marci, L. Palmisano, *Environ. Sci. Technol.* **2001**, *35*, 971–976.
[22] A. Ioannidis, E. Papaconstantinou, *Inorg. Chem.* **1985**, *24*, 439–443.
[23] A. Troupis, A. Hiskia, E. Papaconstantinou, *Angew. Chem.* **2002**, *114*, 1991–1994; *Angew. Chem. Int. Ed.* **2002**, *41*, 1911–1914.
[24] D. Sattari, C. L. Hill, *J. Am. Chem. Soc.* **1993**, *115*, 4649–4657.
[25] R. F. Renneke, M. Kadkhodayan, M. Pasquali, C. L. Hill, *J. Am. Chem. Soc.* **1991**, *113*, 8357–8367.
[26] D. T. Sawyer, J. S. Valentine, *Acc. Chem. Res.* **1981**, *14*, 393–400.
[27] E. Finkelstein, G. M. Rosen, E. J. Rauckman, *J. Am. Chem. Soc.* **1980**, *102*, 4994–4999.
[28] T. Wu, G. Liu, J. Zhao, H. Hidaka, N. Serpone, *J. Phys. Chem. B* **1999**, *103*, 4862–4867.
[29] P. Pichat, C. Guillard, L. Amalric, A-C. Renard, O. Plaidy, *Sol. Energy Mater. Sol. Cells* **1995**, *38*, 391–399.
[30] L. Amalric, C. Guillard, P. Pichat, *Res. Chem. Intermed.* **1994**, *20*, 579–596.
[31] A. Hiskia, E. Papaconstantinou, *Inorg. Chem.* **1992**, *31*, 163–167.
[32] P. Le Magueres, S. M. Hubig, S. V. Lindeman, P. Veya, J. K. Kochi, *J. Am. Chem. Soc.* **2000**, *122*, 10073–10082.
[33] X. M. Zhang, B. Z. Shan, Z. P. Bai, C. Y. You, *Chem. Mater.* **1997**, *9*, 2687–2689.
[34] J. He, J. Zhao, T. Shen, H. Hidaka, N. Serpone, *J. Phys. Chem. B* **1997**, *101*, 9027–9034.
[35] P. V. Kamat, *J. Phys. Chem.* **1989**, *93*, 859–864.
[36] J. Zhao, H. Hidaka, A. Takamura, E. Pelizzetti, N. Serpone, *Langmuir* **1993**, *9*, 1646–1650.
[37] S. Cherian, C. C. Wamser, *J. Phys. Chem. B* **2000**, *104*, 3624–3629.
[38] Y. Tachibana, S. A. Haque, I. P. Mercer, J. R. Durrant, D. R. Klug, *J. Phys. Chem. B* **2000**, *104*, 1198–1205.
[39] C. R. Rice, M. D. Ward, M. K. Nazeeruddin, M. Gratzel, *New J. Chem.* **2000**, *24*, 651–652.
[40] F. Kanoufi, Y. Zu, A. J. Bard, *J. Phys. Chem. B* **2001**, *105*, 210–216
[41] F. Wang, L. M. Sayre, *J. Am. Chem. Soc.* **1992**, *114*, 248–255.
[42] D. C. Duncan, C. L. Hill, *J. Am. Chem. Soc.* **1997**, *119*, 243–244.
[43] R. Neumann, M. Levin, *J. Am. Chem. Soc.* **1992**, *114*, 7278–7286.
[44] C. Venturello, R. D'Aloisio, J. C. J. Bart, M. Ricci, *J. Mol. Catal.* **1985**, *32*, 107–110.
[45] J. Server-Carrio, J. Bas-Serra, M. E. Gonzalez-Nunez, A. Garacia-Gastaldi, G. B. Jamesson, L. C. W. Baker, R. Acerete, *J. Am. Chem. Soc.* **1999**, *121*, 977–984.
[46] L. Cermenati, P. Pichat, C. Guillard, A. Albini, *J. Phys. Chem. B* **1997**, *101*, 2650–2658
[47] X. Li, J. W. Cubbage, T. A. Tetzlaff, W. S. Jenks, *J. Org. Chem.* **1999**, *64*, 8509–8524.
[48] T. Wu, G. Liu, J. Zhao, H. Hidaka, N. Serpone, *New J. Chem.* **2000**, *24*, 93–98.
[49] C. D. Jaeger, A. J. Bard, *J. Phys. Chem.* **1979**, *83*, 3146–3152.
[50] K. Ishibashi, A. Fujishima, T. Watanabe, K. Hashimoto, *J. Phys. Chem. B* **2000**, *104*, 4934–4938.

[51] Y. Nosaka, Y. Yamashita, H. Fukuyama, *J. Phys. Chem. B* **1997**, *101*, 5822–5827.
[52] C. Chen, X. Li, J. Zhao, H. Hidaka, N. Serpone, *J. Phys. Chem. B* **2002**, *106*, 318–324.
[53] C. Rocchiccioli-Deltcheff, M. Fournier, R. Franck, R Thouvenot, *Inorg. Chem.* **1983**, *22*, 207–216.

Received: August 14, 2003
Revised: December 8, 2003 [F5453]

